Test Plan

Wave Energy Power Smoothing Via Supercapacitors Design Comparison

Awardee: Oscilla Power (OPI)

Awardee point of contact: Anna Edwards

Facility: WESRF

Facility point of contact: Ted Brekken

Date: 20 July 2021

EXECUTIVE SUMMARY

This project analyzes two designs of an onboard supercapacitor storage system for a wave energy converter shown in Figure 1.

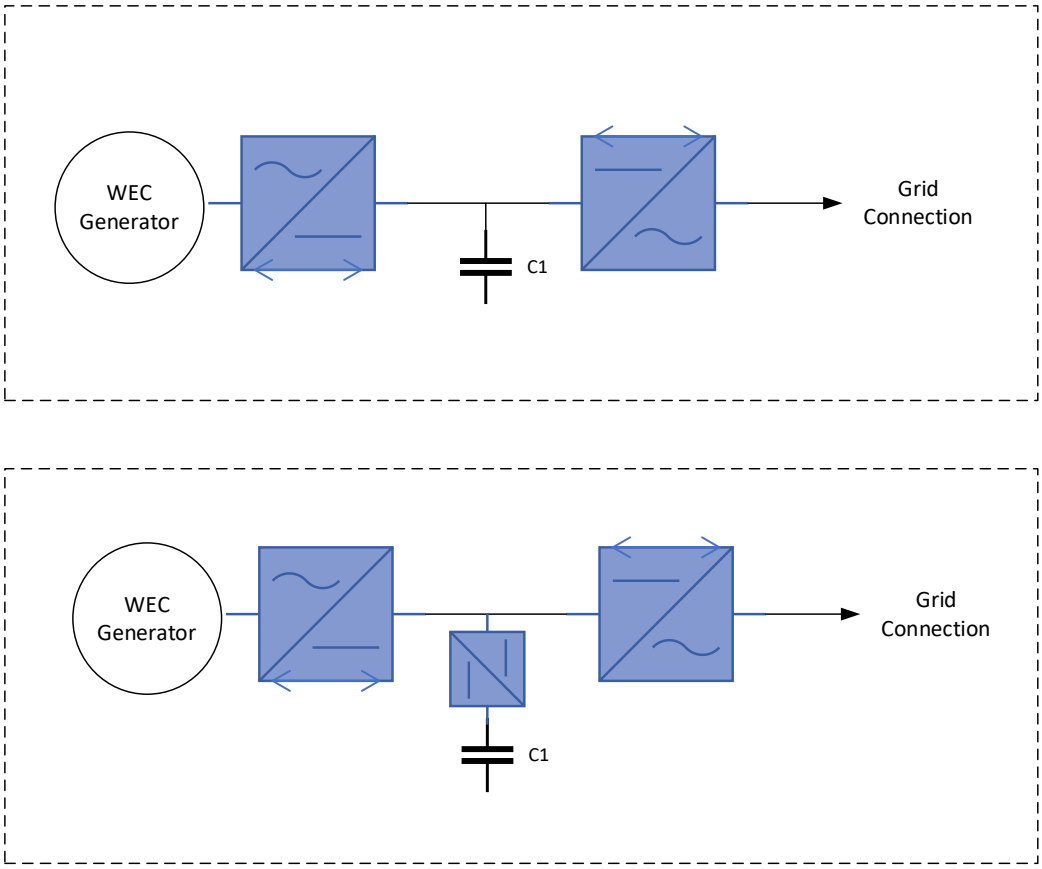

Figure 1: Electrical System one line with two different supercapacitor designs. The top image is for variable bus operation, in which the DC bus between the converters is allowed a significant variation in voltage to utilize the supercapacitor C1. The bottom image is for fixed bus operation, which requires a DC/DC converter to couple supercapacitor C1 to the fixed DC bus.

OSU will provide numerical modeling in WEC-Sim/MATLAB/Simulink of two different designs for a supercapacitor energy storage system for the OPI Triton Wave Energy Converter. Oscilla Power (OPI) will provide one year of wave data that will be run through the two different models. The cost, weight, size, and peak to average power ratio for each design will be compared.

1 INTRODUCTION TO THE PROJECT

This project is focused on validating and optimizing two designs of an onboard supercapacitor storage system and choosing the optimal design for a Wave Energy Converter. The proposed numerical analysis will compare a directly coupled supercapacitor system with a system connected through a DC/DC converter. The peak to average power ratio, cost, and weight of the two systems will be compared to determine the optimal onboard supercapacitor smoothing for a wave energy converter. A reduced peak to average ratio is crucial for Wave Energy Converters to provide the most benefit to the grid.

Supercapacitors are necessary for Wave Energy Converters because of the high peak to average ratio and are the best storage technology for onboard applications. The current supercapacitor design used in the OPI Triton-C that will be deployed in the summer of 2021 at the WETS test site in Hawaii uses a direct coupled Supercapacitor system. When looking at the literature on supercapacitor system all the designs use a DC/DC converter to connect the supercapacitor bank. Since wave energy has a higher peak to average ratio than other technologies the traditional DC/DC converter approach may or may not be the optimal solution. The goal of this research is to determine if our current design is the best approach for our application or if the more traditional system would be better. This research could change or verify the way these systems are currently designed.

2 ROLES AND RESPONSIBILITIES OF PROJECT PARTICIPANTS

OSU will provide numerical modeling in Matlab of two different designs for the supercapacitor systems for the OPI Triton Wave Energy Converter. Oscilla Power will provide one year of wave data that will be run through the two different models. The peak to average ratio for each design will be compared vs the cost and weight of each system. It will be the responsibility of OSU to make sure that limits of the system are maintained, assumptions are noted, and the outputs are reasonable. At the end of the project OSU will provide Oscilla Power with the Matlab files for future analysis.

2.1 APPLICANT RESPONSIBILITIES AND TASKS PERFORMED

- OPI's SBIR phase I (DE-FOA-0001941) determined that an optimum supercapacitor system for the 1MW Triton should be sized to be 3 kWh. This modeling was done using an average power approach for a direct-coupled system.
- OPI has a 1:10 scale lab drivetrain that will be used to generate performance data for this work.
- OPI has completed physical model testing of the Triton architecture at a range of scales from 1:60 to 1:10. We will also complete physical model array tests at 1:50 scale this summer.
- OPI has constructed the Triton C with a direct-coupled supercapacitor system and will test this full-scale system in Hawaii in summer 2021.

2.2 FACILITY RESPONSIBILITIES AND TASKS PERFORMED

- Literature review
- Construction and execution of simulations
- Analysis and interpretation of results

3 PROJECT OBJECTIVES

- Two designs will be tested in simulation: 1) stiff DC bus operation in which the supercapacitor energy storage is connected to a common DC bus through a DC/DC converter that allows for more complete usage of the supercapacitor capacity; 2) variable bus operation, in which the supercapacitors are connected directly to the common DC bus, which requires a varying voltage to charge and discharge the supercapacitors. Design 1 is more complex but allows more full use of the supercapacitors; design 2 is simpler but may require a larger amount of energy storage.
- For each design, the size, weight, cost, and safety considerations will be detailed and compared, including the peak-to-average power ratio, which is an important indicator of overall cost of energy. A table of results will be provided for each of the two designs. The table will include the size, weight, and cost of a candidate specification, along with the measured peak to average power ratio. The size, weight, and cost information will be derived from example hardware already in use by OPI, along with an itemization of comparable equipment available through major commercial sources such as Mouser and DigiKey.

4 TEST FACILITY, EQUIPMENT, SOFTWARE, AND TECHNICAL EXPERTISE

WESRF work will be conducted primarily with WEC-Sim/MATLAB/Simulink, and the models will include the entire power chain from hydrodynamics to converter power to grid power. Modeling will be done at the level of power flow with simplified assumptions of power converter operation and efficiency (i.e., power electronics average modeling). WESRF has access to these computing tools. The work will be conducted by the WESRF director (Ted Brekken) and a graduate research assistant.

5 TEST OR ANALYSIS ARTICLE DESCRIPTION

OPI's Triton WEC (Figure 2), consists of a surface float and vertically asymmetric heave-plate connected by three tendons. It operates in multiple modes of motion (primarily heave and pitch, but also roll, surge and sway), allowing it to capture energy from waves across a wide range of ocean conditions. Drivetrains in the surface float convert the captured mechanical energy into electrical energy with very high efficiency and reliability. Work completed on the Triton has resulted in a simple and efficient marine system, with lower cost and higher reliability than other WECs. Based on extensive numerical modeling, validated by experimental testing across a range of scales from 1:50 through to 1:10, Triton is projected to deliver significantly lower energy costs (LCOE) and higher energy production (AEP) than conventional WECs of the same scale. This statement is validated through Triton's success in the Wave Energy Prize (WEP) competition conducted by the US Department of Energy (DOE) where Triton was one of only 4 systems to exceed the target of 3m/$M for the critical 'ACE' metric, and did so by almost 150%, achieving 4.4m/$M. We have since demonstrated that Triton's performance can be further significantly improved through geometric optimization and advanced controls to achieve an ACE equivalent of 5.6m/$M. Both activities are currently underway through ongoing non-SBIR award funded through the DoE's Office of Energy Efficiency and Renewable Energy (EERE), Water Power Technologies Office

(WPTO) (Contract no: DE-EE0008625). Detailed cost models indicate that Triton can achieve a levelized cost of electricity (LCOE) of under 15¢/kWh at energetic locations worldwide by 2030. Triton's unique features also have the potential to reduce operational and capital expenditures. Specifically, its architecture enables simplified installation procedures, allowing significant reductions in project costs, while a combination of control and load-shedding techniques will maximize survivability, availability and power quality, thereby minimizing operational risk, downtime and costs.

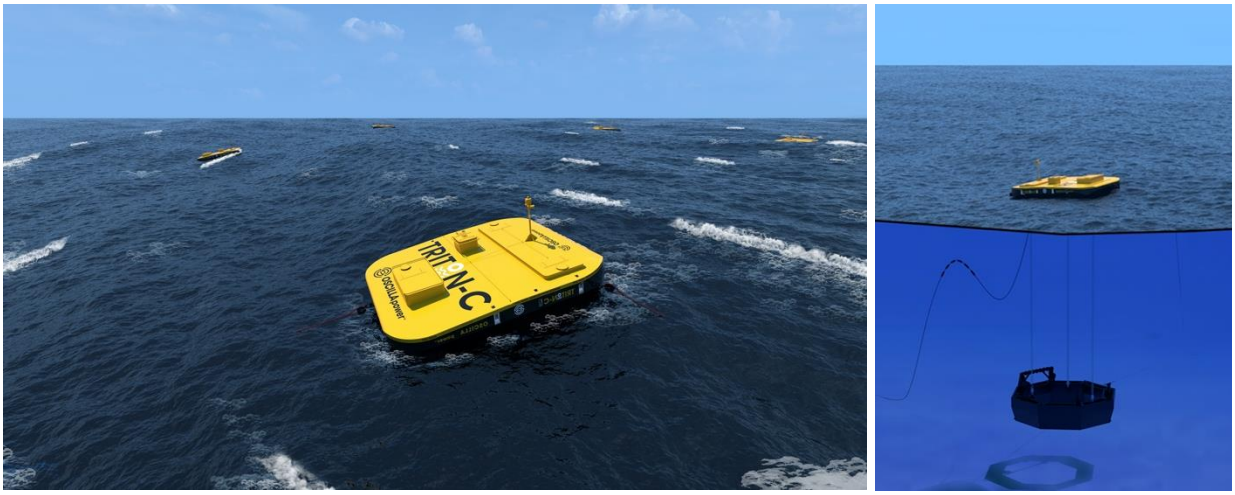

Figure 2: Oscilla Power's Triton Wave Energy Converter

Triton overcomes the limitations of other WECs through:

Increased energy capture: Higher energy capture from waves through multiple excitation modes spread across a wide range of wave periods and higher mechanical to electrical energy conversion efficiency by the linear drivetrain. The Triton's capture width calculations and high ACE value have been independently confirmed by DOE though physical model testing at 1:20 scale.

Reduced capital cost: The use of flexible tendons has a dramatic impact on capital costs due to the elimination of spar-related structural costs. Capital costs are further reduced by the use of low-cost structural materials such as reinforced concrete for the reaction structure.

Extended lifetime: Reduction of tendon or structural failure risk and reduction of extreme loads through a combination of; development and physical testing of novel tendon materials, hydrodynamically-optimized reaction structure design and hydraulic load shedding within the drivetrain.

Reduced transportation/installation cost: Tow-to-site deployment and potential self-deployment using drivetrains will allow for much more versatility and reduced installation cost relative to WECs that rely on seafloor attached or rigid reaction structures.

Survival in Extreme Waves: Through a recently completed EERE-funded Project (DE-EE0007346), OPI demonstrated a survival strategy for the Triton that involves ballasting and partial submergence of the

surface float during extreme waves, allowing power generation to continue. The impact of this strategy is that structural loads can be significantly reduced and kept below design loads for all wave conditions up to a 1:50-year extreme for the US West Coast.

A well-known challenge with wave energy devices is that there is intrinsically a large peak-to-average power variability. Triton has the ability to substantially mitigate this through a number of measures to improve the output power quality and reduce the short-term variability. In the Triton WEC drivetrain a 'power dissipation network' (PDN) is employed to manage mechanical (hydraulic) energy transfer to the electrical generator by eliminating short duration high intensity energy peaks. This allows the peak-to-average ratio to be reduced from a typical maximum of 15:1 to a more manageable 7:1. This corresponds to a substantial reduction in size of the generators and electrical subsystem. Additionally, short term electrical storage in the form of supercapacitors is employed on the output of the generators to reduce short term power variability (variability in the order of seconds) so as to minimize export cable and grid demands.

Hydrostatic hydraulic systems such as that used in the Triton drivetrain are commonly shown to operate at very high efficiency and reliability. An ongoing EERE/WPTO-funded OPI's current DoE project (DE-EE0008387) at OPI focusses on the development and demonstration of this drivetrain, which is currently being assembled in the laboratory. Expected efficiency of the hydraulic system is around 80%, which is comparable to a typical multiple stage rotary gearbox *(typ. 85%)* while the electrical system will show efficiencies in the order of 80-85% due to the near constant speed operation, resulting in drivetrain efficiencies around 70%.

6 Work Plan

1. Literature review
2. WESRF to obtain OPI WEC model information, which includes power time series from OPI experimental and numeric results, and information about power train efficiencies. (It is not anticipated that hydrodynamic information will be necessary for the basic analysis, but should the team decide to recreate OPI system performance given wave information and hydrodynamic data, this will be supplied by OPI.)
3. Build analysis model in WEC-Sim/MATLAB/Simulink which includes the WEC, WEC-side converter, energy storage, grid-side converter, and control
4. Simulate Design 1 *stiff DC bus* for sea states to be specified by OPI.
5. For Design 1, determine the size, weight, cost, and safety considerations including the peak-to-average power ratio.
6. Simulate Design 2 *variable DC bus* for sea states to be specified by OPI.
7. For Design 2, determine the size, weight, cost, and safety considerations including the peak-to-average power ratio.
8. Prepare final report.

6.1 Numerical Model Description

- Modeling and analysis is to be conducted with WEC-Sim/MATLAB/Simulink
- Representative and typical models of energy storage and power converters will be prepared by the WESRF team.
- Oscilla Power will provide generator power output models with half second data.
- WEC-Sim has been validated repeatedly with previous DOE sponsored projects. The energy storage and power converter models are generic and common and represent well known systems.

6.2 Test and Analysis Matrix and Schedule

Task	Due Date
Literature review	Wk 1
WESRF to obtain OPI WEC model information	Wk 2
Build simulation model	Wk 3
Simulate Design 1	Wk 4
Design 1 analysis	Wk 5
Simulate Design 2	Wk 6
Design 2 analysis	Wk 7
Prepare final report	Wk 10

6.3 Safety

NA

6.4 Contingency Plans

No contingencies expected, but in the case of unexpected delays or results, the tasks will be adjusted with input from OPI.

6.5 Data Management, Processing, and Analysis

6.5.1 Data Management

- All work is done with WEC-Sim/MATLAB/Simulink,
- All data is saved in MATLAB format, which can easily be exported to common CSV format upon request.
- All data, notes, and reports will be saved by WESRF on the OSU Box system.
- Test data will be uploaded to MHKDR with a suitable moratorium period.

6.5.2 Data Processing

No data processing required.

6.5.3 Data Analysis

Data includes WEC velocities, forces, and power time-series, and power time-series for the WEC and grid-side converters, and the energy storage. For each of the two designs, a table will be created with several specifications of supercapacitor amount, with the resultant size, weight, cost, and observed peak-to-average ratio of grid power. This will allow OPI to extrapolate to a necessary amount of energy storage for their desired peak-to-average performance.

The final analysis will be a table of cost, weight, size, and peak-to-average power ratio for both designs.

7 PROJECT OUTCOMES

INTRODUCTION

A well-known challenge with ocean wave energy devices is that there is intrinsically large peak-to-average power variability. Ocean wave energy converters (WEC) may employ a hydraulic power dissipation network and onboard energy storage to substantially mitigate the peak-to-average power ratio (PAPR) to improve the output power quality and reduce the short-term variability. Supercapacitors (SC) are a popular choice for energy storage on WECs due to their fast transients, long lifetime, and high power density [1]. The current SC design used in the Triton-C WEC developed by Oscilla Power, Inc. (OPI), deployed in summer 2022 at the WETS test site in Hawaii, uses a direct-coupled SC system. The goal of this research is to determine if a DC/DC converter regulated SC offers benefits over the direct-coupled SC system.

Ocean waves are irregular and slow (e.g., periods of ~10 s) and produce varying power output from the WEC that results in poor coupling with the grid [2]. A standard WEC has a PAPR ratio of 10:1 to 15:1, depending upon the sea tides and weather [3]. A substantial reduction of the PAPR is crucial for WECs to provide the most benefit to the grid. The period and short-term power variability of ocean waves are well-suited for SC-based energy storage, which has a similar high-power charge-discharge period of 1-100 seconds [4],[5].

Many SC-integrated renewable energy systems in the literature use a DC/DC converter to connect the SC bank [5]-[12]. However, converters in the literature are designed for much lower power ratings than a typical WEC of 100s kW to MW levels, requiring larger and more expensive converters. Since a DC/DC converter must be sized for the peak power, the high PAPR of wave energy may cause the traditional DC/DC converter approach to be suboptimal. Little literature exists on WEC PAPR mitigation using a SC directly connected to the DC bus, where one paper focused on lab-based experiments to characterize the SC modules [13]. Additionally, no literature was found comparing these two designs. By performing a direct comparison between these two designs, this research could change or verify the way these systems are currently designed.

This report focuses on validating and sizing two designs of an onboard SC energy storage system to help choose the optimal solution for a WEC. A numerical analysis using field-based data will compare the two designs. Design 1 (Fig. 1a) represents a fixed voltage DC bus operation in which the SC energy storage is

connected to the common DC bus through a DC/DC converter. Design 2 (Fig. 1b) represents a variable voltage bus operation, in which the SC is connected directly to the common DC bus and is currently implemented on the Triton-C. The PAPR, cost, and energy delivered to the grid for the two systems will be compared to determine the preferred onboard SC power-smoothing system for a WEC.

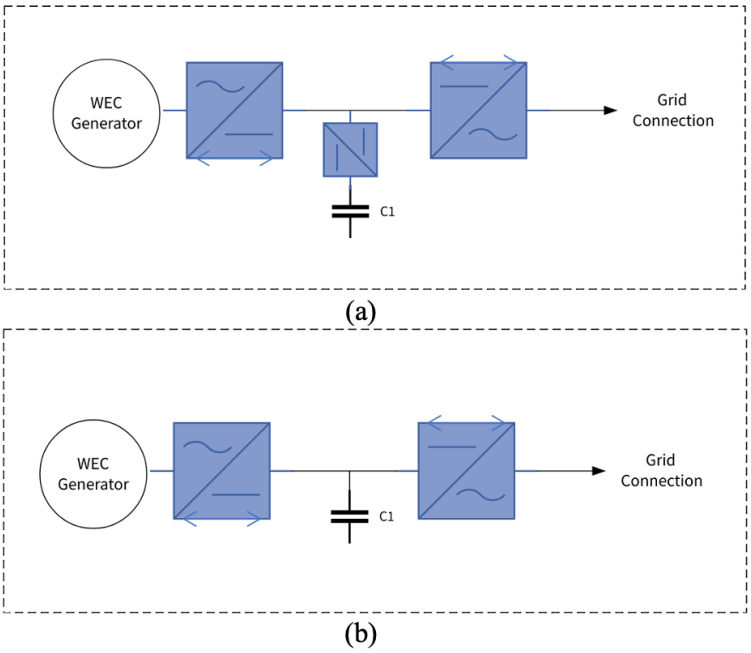

Fig. 1. Electrical system one line for fixed bus operation with (a) DC/DC converter and (b) variable bus operation.

WEC System Modeling

WEC Power Generation

The Triton-C (Fig. 2) consists of a surface float and a vertically asymmetric heave-plate connected by three tendons. It operates in multiple modes of motion (primarily heave and pitch, but also roll, surge and sway), allowing it to capture energy from waves across a wide range of ocean conditions. Drivetrains in the surface float convert the captured mechanical energy into electrical energy with very high efficiency and reliability. OPI has generated their WEC data in OrcaFlex for the dynamics and power, resulting in two different irregular sea states A and B. Sea state A data was generated for a peak period of 7.7 s and a significant wave height of 2.75 m. Sea state B data was generated for a peak period of 14.8 s and a significant wave height of 4.25 m. Both sea states utilize a Bretschneider spectrum to generate the wave profile. The time series power data shown in Fig. 3 is provided as the input to the WEC energy storage system, allowing the hydrodynamics to remain as a black box. The PAPR for sea states A and B of Fig. 3 are approximately 10 and 15, respectively.

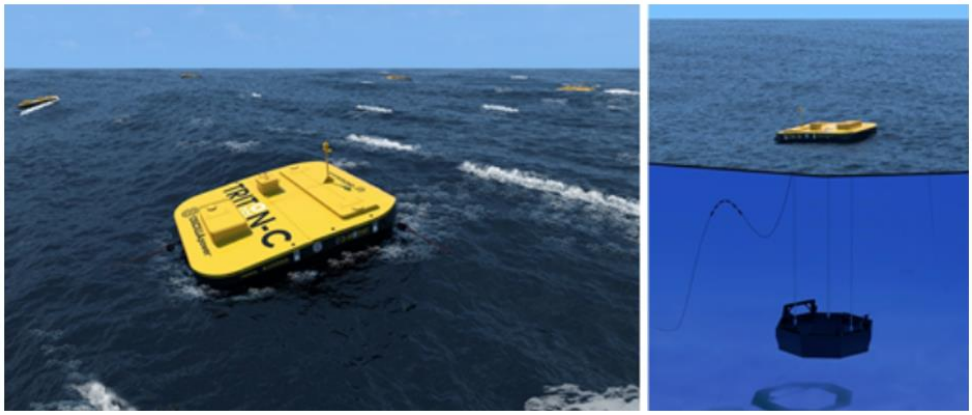

Fig. 2. OPI's Triton-C wave energy converter.

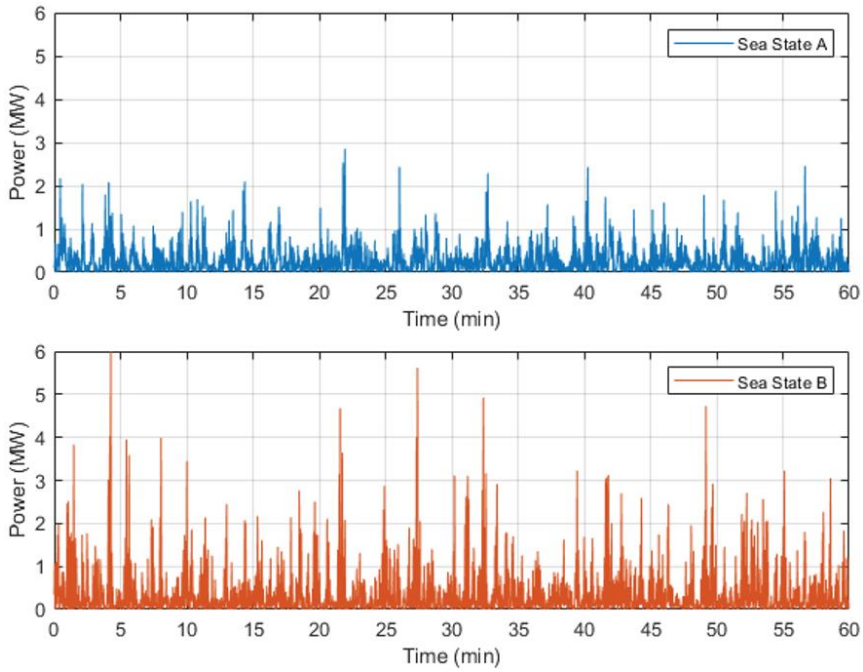

Fig. 3. WEC power time series for sea states A and B

Design 1: Regulated DC Bus

In Design 1, a DC/DC converter regulates the power flow between the DC bus and the SC energy storage (see Fig. 1a). This allows more utilization of the energy stored in the SC in addition to the DC bus voltage to be a design variable, rather than floating with the energy storage. Further discussion on energy storage utilization can be found in Section IV. The generator-side AC/DC converter, energy storage DC/DC converter, and grid-side DC/AC converter are all connected to the common DC bus.

Design 2: Variable DC Bus

Design 2 has the SC energy storage directly connected to the DC bus (see Fig. 1b). While this is a less complex system topology, it also causes the DC bus voltage to vary with the amount of stored energy in the SC. Both the DC/AC and AC/DC converters must then be capable of operating across the entire SC voltage range.

Peak Power Reduction Controls

While the system topologies for Designs 1 and 2 are different, their power flows are effectively the same. This allows the same power controller to be used for both design configurations. The control diagram is shown in Fig. 4. For each design, the power delivered to the grid P_{grid} is the summation of the generated power P_{gen} and power from the energy storage P_{es} (i.e., $P_{grid} = P_{gen} + P_{es}$). Reducing the peak value of P_{grid} is achieved by averaging P_{gen} over a time period of T_w. This time-window averaging unit acts as a low-pass filter using the energy storage to smooth out the generated power waveform. By increasing T_w, P_{gen} is averaged over a longer period which can further smooth out the PAPR of P_{grid}. However, the required energy storage capacity increases with T_w, incurring larger design costs. The power controller also includes a SOC correction factor, which pushes the energy storage SOC to a reference value SOC_{ref} under steady-state conditions. The correction factor time constant τ_{SOC} controls the rate at which the energy storage SOC reaches SOC_{ref}, and is scaled by the max energy capacity of the SC E_{es} to achieve a correction factor in watts.

The proposed power controller could likely be implemented in hardware several different ways. However, one implementation approach will be discussed. For both Design 1 and Design 2, the P_{grid} output of the power controller would serve as an input to a direct power control scheme for the grid-connected DC/AC inverter. In the case of the variable DC bus of Design 2, no additional hardware controls are necessary. The DC/DC controls for Design 1 could simply regulate the DC bus voltage to a constant value. As the input power P_{gen} and output power P_{grid} will affect the DC bus voltage (assuming a DC-link capacitance exists), P_{es} will be implicitly implemented. WEC-side controls are omitted because the WEC-connected AC/DC converter is accounted for in the power generation waveforms discussed previously.

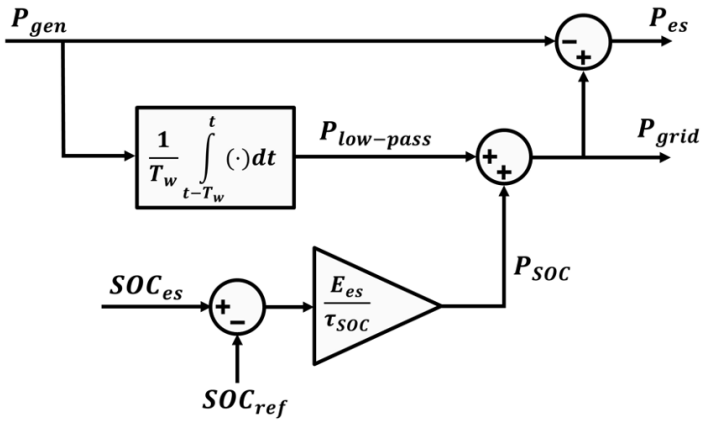

Fig. 4. Power control diagram to distribute WEC generated power between the energy storage and the grid.

Component Models and Sizing

In the context of this design comparison, the system performance and cost using currently available and manufactured equipment is of interest. Since manufacturers rarely reveal converter design details (e.g., semiconductors devices, switching frequency, thermal management, etc.), the use of high-fidelity models that require such information would provide little benefit. Therefore, experimentally-derived or datasheet-based models are used for the SC and inverter. Given the absence of DC/DC converter performance data at the required power ratings of the WEC system, the DC/DC converter is modeled with a constant efficiency of 97%. Section IV includes discussion on how results are impacted by the DC/DC converter model.

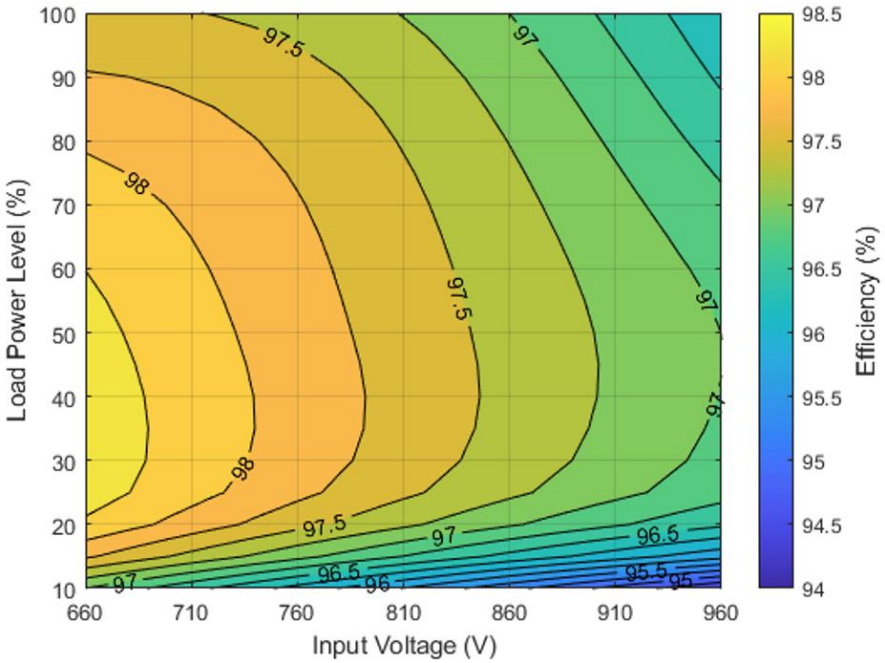

Fig. 5. DC/AC inverter efficiency map dependent on input voltage and normalized power level.

Super Capacitor Model

The SC energy storage is represented by the classic SC model provided in [14] which consists of a single storage element, conduction loss resistance, and self-discharge resistance. The dynamic behavior is dependent on four parameters: rated voltage V_{rated}, total capacitance C, equivalent series resistance R_s, and parallel (self-discharge) resistance R_p. These four parameters are commonly provided in the manufacturer's datasheet, where a SkelMod SMA102V88FAF supercapacitor is used in this paper's study. Scaling of the SC energy capacity is achieved by connecting multiple SC modules in series N_s and parallel N_p, where the total energy capacity is given by

$$E_{es} = N_s \cdot N_p \cdot \frac{1}{2} C V_{rated}^2$$

DC/AC Inverter Model

To model the inverter, an efficiency vs. load and voltage curve is used to calculate realistic losses, implemented as a lookup table for the simulations. The performance data was obtained from the dataset experimentally collected by the California Energy Commission which includes over 3,000 inverters [15]. Performance characteristics were depicted as a function of power level and DC input voltage, providing measurements at three voltage levels and six power levels. Inverters on the list were down-selected to those that met input voltage ranges of 660-960 V (based on system specification) and maximum continuous output power ranges of 300-500 kW. The resulting efficiency map is shown in Fig. 5.

WEC SIMULATIONS

The WEC energy storage optimization presented in this paper considers two design variables: energy storage size E_{es}, and the controller time-window period T_w. Optimal sizing and controller settings are found through an exhaustive search of the design space, sweeping through a range of E_{es} and T_w. The energy storage capacity E_{es} is adjusted by increasing the number of SC modules in parallel N_p while the number of SC modules in series N_s is held constant. Each candidate design is evaluated for total system cost C given a maximum PAPR and various electrical operation constraints, given in Table I. The cost functions are given in the following subsection.

The voltage limits in Table I are the same for every parameter combination as the SC bank voltages are held constant for all designs. Design 1 upper voltage limit is based on the rated voltage of the SkelMod SC, scaled by $N_s = 10$, whereas the lower limit was defined as 20% of the max voltage limit. Design 2 voltage limits are based on the operating range of the DC/AC inverter. The current limits in Table I use the rated current found on the SkelMod SC datasheet scaled by N_p. Using data provided by the industry, this approach can inform engineers on future design improvements of the WEC energy storage system.

TABLE I. DESIGN CONSTRAINTS.

Design	***Constraint***	***Limits***
1	SC bank voltage (V)	$204 \leq V_{es} \leq 1020$
	SC bank SOC	$0 \leq SOC_{es} \leq 1$
	SC bank charge/discharge current (A)	$I_{es} \leq 2689 \cdot N_p$
2	SC bank voltage (V)	$660 \leq V_{es} \leq 960$
	SC bank SOC	$0 \leq SOC_{es} \leq 1$
	SC bank charge/discharge current (A)	$I_{es} \leq 2689 \cdot N_p$

Component Pricing

To evaluate the costs of all electrical components, price models were created using databases for variable frequency drives (VFDs) and SCs. VFDs were used based on the assumption that costs were of similar value to those of WEC-compatible inverters and converters. VFD data was collected for power ratings within 37-372 kW (50-500 HP) among Eaton, Fuji, and Schneider Electric manufacturers [16]. The model is best represented by the linear equation (2), relating price in $ (y) and rated power in kW (x).

$$y = 134x + 1349.3$$

For the SC price model, data was collected with rated voltages equal to or above the already considered 102 V SkelMod SC [17]. Manufacturers included SkelMod, LICAP, and Eaton. The model is best represented by the linear equation (3), relating price in $ (y) and SC energy capacity in Wh (x).

$$y = 30.77x + 324$$

Design Cost and Performance Comparison

Design evaluation is performed in MATLAB/Simulink where Designs 1 and 2 are simulated for both sea states shown in Fig. 3. A total of 800 design variable combinations were simulated for both Design 1 and Design 2 and for both sea states. Energy storage capacity E_{es} ranged from 1 kWh to 20 kWh, and T_w ranged from 1 s to 40 s. Fig. 6 shows the resulting PAPR for all combinations of E_{es}, T_w, sea state, and design configuration. A white cell denotes an infeasible design with too little ES capacity. The control variable T_w has the greatest impact on PAPR, since it affects the power averaging of the energy storage. The capacity E_{es} then correlates to how large a T_w can be used. This is attributed to the averaging approach used in the peak power reduction controller.

The major benefit of Design 1 is the decoupling of the inverter input voltage range and the SC voltage. This allows greater utilization of the energy storage, where 96% of the available energy storage is used. Whereas Design 2 utilizes only 52.7%. The greater energy storage utilization of Design 1 over Design 2 can also be observed in Fig. 6. For the same T_w, Design 1 requires approximately half of the energy storage size as Design 2 for both sea states.

Table II summarizes the results of the lowest cost configurations for each design and sea state, while achieving a $PAPR < 3$ and $PAPR < 5$. Note that the PAPR values are not exactly the same for each design configuration. Since the PAPR does not monotonically decrease with an increasing T_w, it is possible for a design with a lower PAPR to be cheaper than a design with a higher PAPR. The PAPR limits selected for Table II are just samples to provide a more in-depth quantitative comparison between the two design comparisons. Ultimately the PAPR limit would be discussed with the local utility company to determine the optimal PAPR for grid services.

While Design 2 utilizes around 50% of the available energy stored in the SC, it actually is the cheaper design option. This is observed in Table II. Since Design 2 does not include a DC/DC converter, the overall system cost is less than Design 1. Even though Design 2 requires 2-4 times the energy storage capacity of Design 1, the lower cost of energy storage is not enough to compensate for the cost of the DC/DC converter. The cost difference for the same PAPR can also be inferred from Fig. 7, which shows the PAPR vs. total system cost for Designs 1 and 2. Interestingly, the PAPR rate of change over cost is overall more

gradual for Design 2 than Design 1. This suggests there exists a PAPR where Design 1 becomes the more cost-effective option – provided the intersection occurs before unity PAPR.

The total energy delivered to the grid E_{grid} is another important detail to consider, and is included in Table II. Simulating Design 2 results in an E_{grid} 3% larger than Design 1. Note that this exact difference is not entirely accurate due to the fixed-efficiency DC/DC converter model used. However, it can be concluded that no DC/DC converter will result in a higher E_{grid}. While Design 1 enables the inverter to operate with its maximum efficiency input voltage, the *total* system efficiency must be greater than Design 2 for a higher E_{grid}. To achieve a higher total efficiency than Design 2, the DC/DC converter would require an efficiency >99% at all operating points, which is likely infeasible or impractical in practice.

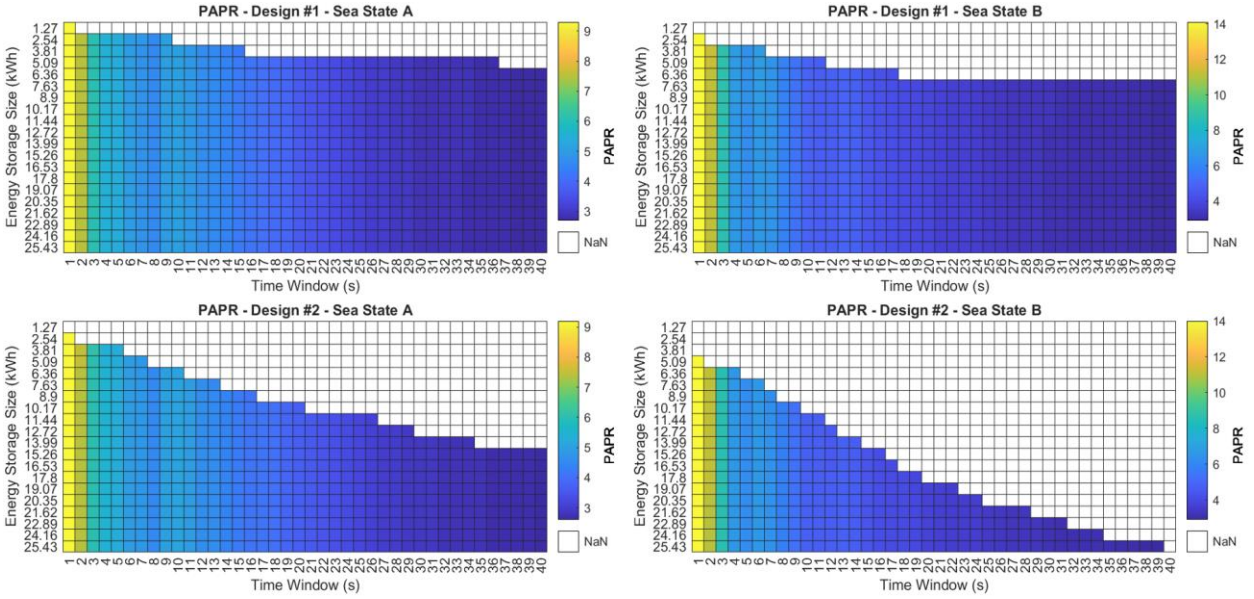

Fig. 6. Maximum PAPR vs E_{es} and T_w for both design configurations and sea states.

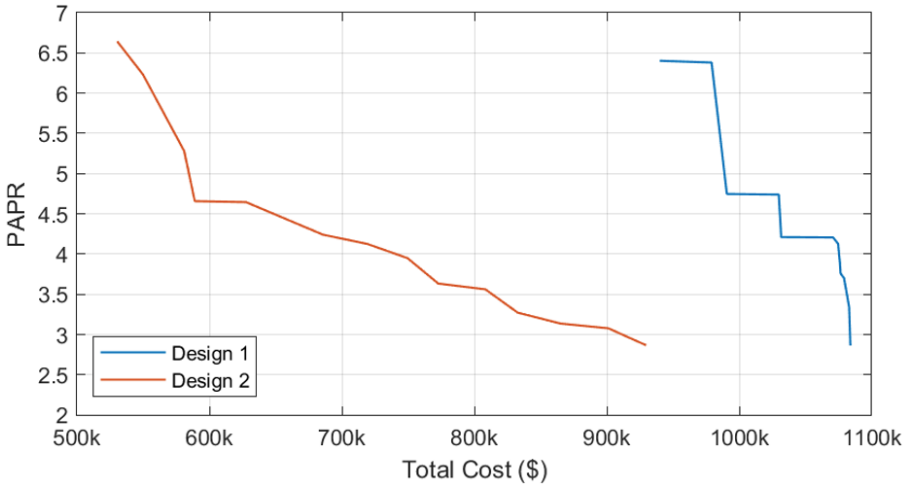

Fig. 7. PAPR vs total system cost of Designs 1 and 2 for sea state B.

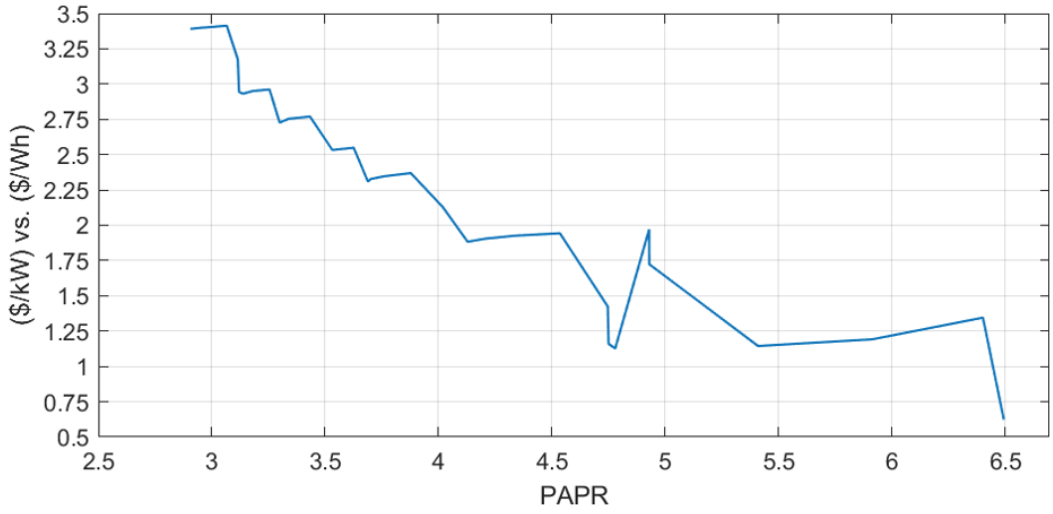

Fig. 8. The ratio between the $/kW of the DC/DC converter and $/Wh of the SC energy storage where the costs of design 1 and 2 are equivalent. The plot shows the ratio for a range of PAPR for sea state B. The price models presented in this paper result in a cost ratio of 4.36.

TABLE II. TOP CONFIGURATIONS FOR DESIGNS 1 AND 2 FOR $PAPR < 3$ AND $PAPR < 5$.

Sea State	*Design*	*PAPR*	*Total Cost ($)*	*SC Cost ($)*	*DC/AC Cost ($)*	*DC/DC Cost ($)*	T_w *(s)*	E_{es} *(kWh)*	E_{grid} *(kWh)*
A	1	2.86	561k	157k	106k	298k	34	5.09	273
		4.62	508k	79k	170k	259k	8	2.54	272
	2	2.92	502k	392k	110k	-	29	12.72	279
		4.78	336k	157k	179k	-	7	5.09	277
B	1	2.91	1084k	235k	144k	705k	39	7.63	367
		4.75	991k	157k	234k	600k	11	5.09	366
	2	2.87	930k	783k	147k	-	39	25.43	379
		4.66	589k	352k	237k	-	11	11.44	377

Alternative Component Pricing Analysis

The results in Table II and in Fig. 7 are largely dependent on the cost models used, which are based on prices provided by online distributors gathered at the time of writing. These prices are likely subject to change in the future when the manufacturing of power electronics and SC becomes more cost efficient. Additionally, working directly with a power converter manufacturer could result in lower costs. To accommodate for these uncertainties, an alternative component pricing analysis is performed. The goal is to determine at what point does Design 1 have an equivalent cost to Design 2 for different DC/DC converter and SC price models. The change in pricing models is represented by a ratio between DC/DC converter $/kW and SC energy storage $/Wh. The AC/DC converter costs are similar between both designs and are thus omitted from this analysis.

For a range of PAPR, the $/kW vs. $/Wh ratio where Design 1 has an equivalent cost to Design 2 is shown in Fig. 8. This considers only sea state B as it has a higher initial PAPR. For reference, the $/kW vs. $/Wh ratio of the price models (1)-(2) presented in this paper is 4.36. Hence, for all PAPR, Design 1 is more costly. However, if the $/kW vs. $/Wh ratio drops below 2.5, for example, then Design 1 with DC-DC converter will be cheaper if PAPR is required to be less than 3.5. Again, the non-monotonicity of the PAPR for an increasing T_w causes the plot of Fig. 8 to also be non-monotonic. There is a general trend that a lower PAPR requires a smaller reduction in DC/DC converter cost (with respect to the SC cost) for Design 1 to become the cheaper option. This was also inferred from Fig. 7, where the cost difference between the two designs is reduced as the PAPR decreases. However, Fig. 8 provides a more concise analysis quantifying the necessary component prices for the preferred design to become Design 1.

7.1 Lesson Learned and Test Plan Deviation

The analysis went smoothly and there were no deviations or surprises in the test plan.

8 Conclusions and Recommendations

This report presented a design comparison between two WEC energy storage configurations that focused on the PAPR and total system cost. Design 1 uses a DC/DC converter to regulate the energy stored in the SC and the DC bus voltage. Design 2 has the SC connected directly to the DC bus, and is the current design of OPI's Triton-C WEC. Both designs were evaluated through simulations using industry-based data. While the use of a DC/DC converter can result in higher utilization of the SC energy capacity, the cost of a DC/DC converter outweighs the savings in SC size. Additionally, the analysis concludes that Design 2 has a greater total system efficiency.

9 References

[1] J. H. Prudell, A. Schacher, and K. Rhinefrank, "Direct drive ocean wave energy electric plant design methodology," in *Oceans*, 2012, pp. 1-7.

[2] B. Czech and P. Bauer, "Wave Energy Converter Concepts: Design Challenges and Classification," in *IEEE Industrial Electronics Magazine*, vol. 6, no. 4, pp. 4-16, 2012.

[3] Y.H Yu, E. Muljadi, and H. B. Karayaka, "Investigations into Balancing Peak-to-Average Power Ratio and Mean Power Extraction for a Two-Body Point-Absorber Wave Energy Converter," in *Advanced Analysis and Techniques of Wave Energy Conversion and Integrated Storage*, vol. 14, no. 12, 2021.

[4] A. Rufer, *Energy Storage: Systems and Components*, Boca Raton, FL, CRC Press, 2017, pp. 108-109.

[5] I. H. Panhwar, K. Ahmed, M. Seyedmahmoudian, A. Stojcevski, B. Horan, S. Mekhilef, A. Aslam, and M. Asghar, "Mitigating Power Fluctuations for Energy Storage in Wind Energy Conversion System Using Supercapacitors," in *IEEE Access*, vol. 8, no. 1, pp.189747-189760, 2020.

[6] S. Hazra and S. Bhattacharya, “Minimizing Reactive Current of a High Gain Dual Active Bridge Converter for Supercapacitor Based Energy Storage System Integration,” in *Proc. IEEE Energy Conversion Congress and Exposition (ECCE)*, 2018, pp. 1-8.

[7] P. Moreno-Torres, M. Blanco, G. Navarro, and M. Lafoz, “Power smoothing system for wave energy converters by means of a supercapacitor-based energy storage system,” in *Proc. European Conference on Power Electronics and Applications*, 2015, pp. 1-7.

[8] P. Bauer, J. A. Ferreira, R. Kessel, and K. T. Todorčević, “Bidirectional modular multilevel DC-DC converter control and loss modeling for energy extraction from Electro Active Polymer Wave Energy generator,” in *Proc. IEEE ECCE Asia Downunder*, 2013, pp. 1-7.

[9] F. Xue, R. Yu, W. Yu, A. Q. Huang, and Y. Du, “A novel bi-directional DC-DC converter for distributed energy storage device,” in *Proc. IEEE Applied Power Electronics Conference and Exposition (APEC)*, 2015, pp. 1-5.

[10] J.S. Artal-Sevil, J.A. Domínguez-Navarro, D. Martínez, and C. Bernal-Ruíz, “Control and Design of an IPOS DC-DC Converter applied to High Voltage DC Transmission in a Wave Energy Converter,” in *Proc. Fourteenth International Conference on Ecological Vehicles and Renewable Energies (EVER)*, 2019, pp. 1-9.

[11] G. Rajapakse, S. Jayasinghe, A. Fleming, and M. Negnevitsky, “Grid Integration and Power Smoothing of an Oscillating Water Column Wave Energy Converter,” in *Energies*, vol. 11, no. 7, pp. 1-19, 2018.

[12] D. Murray, M. Egan, J. Hayes, D. Sullivan, “Applications of Supercapacitor Energy Storage for a Wave Energy Converter System,” in *Proc. European Wave and Tidal Energy Conference (EWTEC)*, 2009, pp. 1-10.

[13] D. B. Murray, J. G. Hayes, D. L. O'Sullivan and M. G. Egan, “Supercapacitor Testing for Power Smoothing in a Variable Speed Offshore Wave Energy Converter,” in *IEEE Journal of Oceanic Engineering*, vol. 37, no. 2, pp. 301-308, 2012.

[14] L. Zhang, Z. Wang, X. Hu, F. Sun, and D. G. Dorrell, “A comparative study of equivalent circuit models of ultracapacitors for electric vehicles,” in *Journal of Power Sources*, vol. 274, pp. 899-906, 2015.

[15] California Energy Commission, “Solar Equipment Lists”, 2020. Accessed on: Jan. 5th, 2022. [Online]. Available: https://www.energy.ca.gov/programs-and-topics/programs/solar-equipment-lists

[16] Grainger, “Variable Frequency Drives”, 2022. Accessed on: Jan. 7, 2022. [Online]. Available: https://www.grainger.com/category/motors/motor-drives-speed-controls/variable-frequency-drives-accessories/variable-frequency-drives

[17] Digi-Key Electronics, “Electric Double Layer Capacitors (EDLC), Supercapacitors”, 2022. Accessed on: Jan. 7, 2022. [Online]. Available: https://www.digikey.com/en/products/filter/electric-double-layer-capacitors-edlc-supercapacitors/61

10 ACKNOWLEDGEMENTS

The authors wish to thank the TEAMER program for enabling this project.

● APPENDIX